Applied Radiation and Isotopes 70 (2012) 1624–1631

Contents lists available at SciVerse ScienceDirect

Applied Radiation and Isotopes

journal homepage: www.elsevier.com/locate/apradiso

# Investigation of 3′-debenzoyl-3′-(3-([$^{124}$I]-iodobenzoyl))paclitaxel analog as a radio-tracer to study multidrug resistance in vivo

M. Sajjad [a,*], U. Riaz [a], R. Yao [a], R.J. Bernacki [b], M. Abouzied [a], D.A. Erb [a], N.D. Chaudhary [b], J.M. Veith [b], G.I. Georg [c], H.A. Nabi [a]

[a] Department of Nuclear Medicine, State University of New York, Buffalo, New York, USA
[b] Pharmacology and Therapeutics, Roswell Park Cancer Institute, Buffalo, New York, USA
[c] Department of Medicinal Chemistry, Institute for Therapeutics Discovery and Development, University of Minnesota, Minneapolis, Minnesota, USA

ARTICLE INFO

*Article history:*
Received 22 December 2010
Received in revised form
9 February 2012
Accepted 5 March 2012
Available online 24 March 2012

*Keywords:*
Iodine-124
Paclitaxel
Taxol
P-glycoprotein
Tumor

ABSTRACT

A study was carried out to identify a suitable radioactive paclitaxel analog and to use it to investigate tumor multidrug resistance in vivo. 3′-Debenzoyl-3′-(3-([$^{124}$I]-iodobenzoyl))paclitaxel was prepared by aromatic iodination of 3′-debenzoyl-3′-(3-trimethylstannylbenzoyl)paclitaxel. Uptake of the labeled paclitaxel analog in nude mice bearing tumor with the paclitaxel sensitive cancer cell lines MCF7 and MDA-435/LCC6(WT), and multidrug resistant cell lines NCI/ADR-RES and MDA-435/LCC6(MDR), was studied. There was no difference in drug level between the sensitive and resistant MDA-435/LCC6 tumors at 6 h post-injection. However, at 6 h, there was a significant increase in drug level for the MCF7 tumor as compared with the NCI/ADR-RES tumor, presumably due to increased drug retention. At 24 h, drug uptake/retention was significantly higher in both sensitive tumor cell lines as compared to their drug resistant counterparts. Pretreatment of mice with MDR transport modulators, Cyclosporine or tRA 96029, did not increase the level of labeled paclitaxel analog in the drug resistant MDA-435/LCC6(MDR) tumor. On the other hand, at 24 h Cyclosporine apparently increased analog level in the drug sensitive MDA-435/LCC6(WT) tumor, aiding drug imaging studies.



## 1. Introduction

The taxoids paclitaxel and docetaxel (Fig. 1) are primary tubulin-targeting drugs in the treatment of human cancers, particularly breast, ovarian, and lung carcinomas. Their effectiveness in cancer chemotherapy is often limited because of tumor drug resistance, which causes short duration tumoricidal response. Possible mechanisms underlying tumor drug resistance include over-expression of the mdr1 gene and increased levels of membrane glycoprotein P-170 (Pgp), an ATP-dependent transport pump capable of effluxing these drugs (Gottesman et al., 2002).

Early diagnosis of tumors that are resistant to paclitaxel or docetaxel and identification of the underlying mechanisms of resistance are critical pieces of information that would enable the adjustment of therapeutic strategies if available before initiation of treatment (individualized medicine). The available therapeutic options include (1) the use of drugs that are not substrates for Pgp (e.g., Cisplatin), (2) the use of second generation taxoids with higher therapeutic efficacy against multidrug resistant tumors (e.g. IDN 5109, see Vredenburg et al., 2001), and (3) the use of drug resistance reversal agents (e.g., tRA 98006, see Brooks et al., 2003).

Radiotracer based molecular imaging with positron emission tomography (PET), single photon emission computer tomography (SPECT), and gamma camera are effective technologies for monitoring tumor drug uptake and retention (Phelps, 2000). Li et al. (1997) synthesized and injected indium-111-DTPA-paclitaxel into mice implanted with MCA-4, a paclitaxel responsive mammary tumor. The drug was selectively taken up by the tumor with tumor to muscle drug ratios of 2.64, 3.16 and 6.94 at 30 min, 2 h and 24 h, respectively, although the absolute uptake in the tumor decreased from 1.95% (injected dose/g) at 30 min to 0.21% at 24 h after injection. Gamma scintigraphy and autoradiographic studies showed retention of radiolabeled paclitaxel in the tumor up to 24 h after injection. Two major limitations of an indium-111 labeled agent are (1) its high rate of accumulation in the liver, rendering the evaluation of hepatic metastases quite difficult; and (2) its known high affinity for transferrin receptors, leading to excessive radiation burden to the bone marrow.

Hendrikse and Vaalburg (2002) developed a method that uses [$^{11}$C]-Verapamil as a positron emitting Pgp substrate to measure the Pgp functionality in vivo with PET. They reported that the [$^{11}$C]Verapamil accumulation at 1 h post-injection in the lungs, heart and tumor was 43, 1.3, and 0.9% respectively, of the total injected dose. The drawback of this tracer is that the high lung uptake would interfere with any breast tumor imaging protocol.

* Correspondence to: Department of Nuclear Medicine, SUNY University at Buffalo, 105 Parker Hall South Campus, 3435 Main St., Buffalo NY 14214, USA. Tel.: +716 838 5889.
*E-mail address:* msajjad@buffalo.ed (M. Sajjad).

0969-8043/$ - see front matter © 2012 Elsevier Ltd. All rights reserved.
http://dx.doi.org/10.1016/j.apradiso.2012.03.008

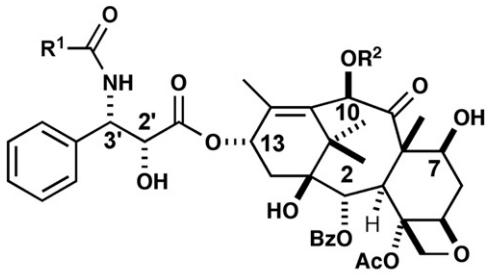


**Paclitaxel $R^1$ = Ph, $R^2$ = Ac**
**Docetaxel $R^1$ = O-tert-butyl, $R^2$ = H**

**Fig. 1.** Structures of paclitaxel and docetaxel.

3′-Debenzoyl-3′-(4-([$^{123}$I]-iodobenzoyl))paclitaxel as an agent for tumor drug resistance screening has been previously reported by Roh et al. (2000). However, its usefulness to image Pgp was not studied. Kiesewetter et al. (2003) reported the synthesis and preliminary evaluation of paclitaxel derivatives labeled with $^{18}$F, $^{76}$Br, and $^{124}$I. They concluded that the increase of [$^{18}$F]-paclitaxel accumulation in liver and lungs after administration of the Pgp-inhibitor XR9576 is related to Pgp inhibition and hence it is a useful agent for PET imaging of the dynamic of Pgp expression. Roh et al. (2000) and Kiesewetter et al. (2003) have prepared labeled paclitaxel with $^{123}$I and $^{124}$I at the para position respectively. These drugs were not studied in tumor bearing mice. Kiesewetter et al. (2003) used Sprague-Dawley rats for biodistribution studies. In addition the effect of preadministration of paclitaxel on the biodistribution was also studied. Preadministration of paclitaxel prior to $^{124}$IPAC resulted in significantly increased uptake in lung and liver. It was concluded that there Pgp has a role in lung uptake. The higher liver uptake was attributed to enhanced metabolism upon preadministration of paclitaxel. Because of the existence of multiple iodine isotopes, development of paclitaxel derivatives labeled with iodine allows the use of multiple molecular imaging modalities (PET, SPECT and gamma camera) and selection from a wide range of radioisotope half-life for monitoring the drug uptake. We expected a possible negative pharmacological effect by introducing an iodo group on the 3′-phenyl ring. Therefore, we synthesized three iodo isomers of paclitaxel (i.e., 3′-debenzoyl-3′-(2, 3, and 4-iodobenzoyl)paclitaxel). The isomer that was most similar to paclitaxel in the cytotoxicity assays was iodo at 3-position and therefore was chosen for labeling. Bio-distribution studies were performed in mice bearing tumors, using $^{124}$I-labeled drug. These mice were also sequentially imaged with a microPET camera after the injection of $^{124}$I-labeled drug. The performance of the iodo isomers of paclitaxel and paclitaxel were assessed with MCF7, NCI/ADR-RES and MDA-435/LCC6(WT)/MDA-435/LC6(MDR) tumor cell lines. The bio-distribution and PET imaging studies were performed with labeled 3′-debenzoyl-3′-(3-([$^{124}$I]-iodobenzoyl))paclitaxel in nude mice bearing MCF7, NCI/ADR-RES and MDA-435/LCC6(WT)/MDA-435/LC6(MDR) tumors. As a useful application of these tracers, we evaluated the effectiveness of two modulators, Cyclosporine and tRA 96023 on radiotracer uptake in Pgp sensitive and resistant tumors.

## 2. Experimental

### 2.1. Materials and methods

All chemical reactions were performed under an argon atmosphere. All air and moisture sensitive reactions were conducted using Schlenk glassware using standard inert atmosphere techniques. Thin layer chromatography (TLC) was performed on Merck Silica Gel 60$F_{254}$ silica plates and visualized by UV illumination. Flash column chromatography was performed on Merck silica gel. $^1$H or $^{13}$C NMR spectra were recorded using a Varian VXR-500 and 400 NMR in deuterated solvents as indicated in the experimental data. Mass spectral determinations were carried out at 70 eV. All organic reagents and anhydrous solvents were purchased from Aldrich Chemical Company and were used without further purification. Baccatin III was purchased from Dabur India Limited, Ghaziabad, India. Iodine-124 was produced by the $^{124}$Te(p,n)$^{124}$I reaction and was purified by dry distillation (Sajjad et al., 2006). Enriched Tellurium-124 dioxide was used as a target. IODO-GEN coated tubes were purchased from Pierce Biotechnology. HPLC was carried out on a system comprised of a Chrom Tech Iso-2000 pump, Hitachi L-4000 UV detector and a CsI(Tl) radiation detector. The detectors were connected via HP35900E interface to a computer with HP Chemstation software. The HPLC eluent was monitored simultaneously with a UV detector (230 nm) and a radioactivity detector. For radiolabeled compounds, the TLC was analyzed on a Bioscan 200 TLC scanner. Radioactivity was measured in a Capintec dose calibrator.

### 2.2. Human tumor cell lines

The MCF7-S and NCI/ADR-RES carcinoma cell lines were purchased from the American Type Culture Collection (ATCC). The MDA-435/LCC6(WT) and MDA-435/LCC6(MDR) cell lines were provided by Dr. R. Clarke, Lombardi Cancer Center, Georgetown University, School of Medicine. Cell lines were propagated as monolayers in RPMI-1640 containing 5% FCS, 5% NuSerum IV, 20 mM HEPES, 2 mM L-glutamine at 37 °C in a 5% $CO_2$ humidified atmosphere. The doubling times for the cell lines range between 20 and 30 h.

### 2.3. Growth inhibition assay in 96 well microtiter plates

Assessment of cell growth inhibition was determined according to the methods of Skehan et al. (1990). Briefly, cells were plated between 800 and 1500 cells/well in 96 well plates and incubated at 37 °C for 15–18 h prior to drug addition to allow cell attachment. Compounds to be tested were solubilized in 100% DMSO and further diluted in RPMI-1640 containing 10 mM HEPES. Each cell line was treated with 10 concentrations of compound (five log range). After 72 h incubation, 100 μL of ice-cold 50% trichloroacetic acid was added to each well and incubated for 1 h at 4 °C. Plates were then washed five times with tap water to remove the trichloroacetic acid, low-molecular-weight metabolites and serum proteins. 50 μl of 0.4% sulforhodamine B (SRB), an anionic protein stain, was added to each well. SRB staining changes linearly with increases or decreases in number of cells and protein concentrations. These staining characteristics provide an accurate assessment of cell growth. Following 5 min incubation at room temperature, plates were rinsed five times with 0.1% acetic acid and air-dried. Bound dye was solubilized with 10 mM Tris Base (pH 10.5) for 5 min on a gyratory shaker. Optical density was measured at 570 nm.

## 3. Biodistribution and imaging

Female nude athymic mice, 6–10 weeks of age obtained from National Cancer Institute (Fredrick, MD). Animals were housed at the Medical Research Complex at Roswell Park Cancer Institute. Animal care was within IACUC guidelines and meets all Federal and State regulation. Mice were tumored subcutaneously,

bilaterally with resistant variant on the right shoulder area and wild type tumor on the left, either MCF7 paired with its resistant variant NCI/ADR-RES or MDA-435/LCC6(WT) paired with MDA-435/LCC6(MDR). Two million cells per sc implant were used. Mice were imaged when tumors reached an average tumor volume of 100 $mm^3$, 7–10 day post implant. Sixteen nude mice were used for biodistribution studies with MDA-435/LCC6(WT) and MDA-436/LCC6(MDR) tumors. Each time point is average of four mice. Fourteen nude mice were used for obtaining biodistribution data with MCF7 and NCI/ADR-RES tumors. Three mice were used for 0.5, 2 and 6 h time points, whereas for the 24 h time point five mice were used. 100–200 μl solution of the labeled drug, formulated in a saline: Cremophor: ethanol (5:0.5:0.5) mixture, was injected via the tail vein. Mice were anesthetized by continuous inhalation of 2% isofluorane and imaged for 30 min at 5 min, 8 h, and 24 h post-injection using microPET Focus120. The mice were imaged in a prone position. Mice were euthanized for tissue biodistribution studies by intra-peritoneal administration of sodium pentobarbital. Organs were harvested and weighed. The radiation intensity of each tissue was counted using a gamma counter, and the percentage of injected dose per gram (% ID/g) of tissue was calculated by comparing with the standard sample.

## 4. Data analysis

Data were fit with the Sigmoid-Emax concentration-effect model (Holford and Scheiner, 1981) with nonlinear regression, weighted by the reciprocal of the square of the predicted response. The fitting software was developed at RPCI with Microsoft FORTRAN, and uses the Marquardt (1963) algorithm as adapted by Nash (1979) for the nonlinear regression. The concentration of drug, which resulted in 50% growth inhibition ($IC_{50}$), was calculated.

## 5. Synthesis

### 5.1. 3′-Debenzoyl-7-(trichloroethoxycarbonyl)paclitaxel (2)

The baccatin III-coupled product **1** (111.4 mg, 0.107 mmol), prepared using the method by Reddy et al. (2001), was dissolved in formic acid (96%, 4.6 mL) and stirred at room temperature for 2 h. The solvent was evaporated under *vacuo* and the residual solid was dried under high vacuum. The crude free amine was used for the next step without further purification.

### 5.2. 3′-Debenzoyl-3′-(4-iodobenzoyl)-7-(trichloroethoxycarbonyl)paclitaxel (3a)

The crude amine **2** (111 mg, 0.107 mmol) was dissolved in EtOAc (3.0 mL) and then a saturated solution of aq. $NaHCO_3$ (3.0 mL) was added and the reaction mixture was stirred for 5 min at room temperature. To the resulting mixture was added dropwise 4-iodobenzoyl chloride (31.4 mg, 0.118 mmol) at 0 °C. TLC monitoring indicated reaction completion after 15 min. The reaction mixture was diluted with EtOAc (2.0 mL). The organic layer was washed with brine, dried over $MgSO_4$, filtered and concentrated under reduced pressure. The residual solid was used for the next step without further purification.

### 5.3. 3′-Debenzoyl-3′-(3-iodobenzoyl)-7-(trichloroethoxycarbonyl)paclitaxel (3b)

Compound **3b** was prepared using the method described for **3a** and was used for the next step without further purification.

### 5.4. 3′-Debenzoyl-3′-(2-iodobenzoyl)-7-(trichloroethoxycarbonyl)paclitaxel (3c)

Compound **3c** was obtained using the method described for **3a** and was used for the next step without further purification.

### 5.5. 3′-Debenzoyl-3′-(4-iodobenzoyl) paclitaxel (4a)

To a stirred solution of **3a** (111.5 mg, 0.099 mmol) in tetrahydrofuran (17 mL) and MeOH (17 mL) was added $NH_4OAc$ (61.0 mg, 0.794 mmol). The reaction mixture was stirred at room temperature for 5 h and then diluted with EtOAc, washed with brine, dried over $MgSO_4$, filtered and concentrated under *vacuo*. The crude residue was purified via flash silica gel column chromatography. Elution with 20–50% EtOAc/hexanes afforded compound **4a** as a white solid (65.1 mg) in 67% yield. $^1$H NMR (500 MHz, $CDCl_3$) $\delta$ 1.14(*s*,3H), 1.23 (*s*, 3H), 1.68 (*s*, 6H), 1.78 (*s*, 3H), 1.84–1.90 (*m*, 1H), 2.23 (*s*, 3H), 2.36 (*s*, 3H), 2.25–2.34 (*m*, 1H), 2.49–2.56 (*m*, 1H), 3.58 (*d*, $J$=4 Hz, 1H), 3.79 (*d*, $J$=6.5 Hz, 1H), 4.18 (*d* of AB *q*, $J$=8.5 Hz, 1H), 4.30 (*d* of AB *q*, $J$=8.5 Hz, 1H), 4.37–4.40 (*m*, 1H), 4.77 (*dd*, $J$=4.5, 2.5 Hz, 1H), 4.92 (*d*, $J$=8 Hz, 1H), 5.66 (*d*, $J$=7 Hz, 1H), 5.75–5.77 (*m*, 1H), 6.19 (*t*, $J$=9 Hz, 1H), 6.26 (*s*, 1H), 6.99 (*d*, $J$=9 Hz, 1H), 7.33–7.52 (*m*, 9H), 7.60–7.63 (*m*, 1H), 7.72 (*d*, $J$=9 Hz, 2H), 8.12 (*d*, $J$=7.5 Hz, 2H); HRMS *m*/*z* calculated for $C_{47}H_{50}O_{14}NINa$: 1002.2168. Found: 1002.2185.

### 5.6. 3′-Debenzoyl-3′-(3-iodobenzoyl)paclitaxel (4b)

To a stirred solution of **3b** (85.6 mg, mmol) in tetrahydrofuran (13 mL) and MeOH (13 mL) was added $NH_4OAc$ (64.3 mg, 0.835 mmol). Upon completion of the reaction after stirring for 5 h at room temperature, the mixture was diluted with EtOAc, washed with brine, dried over $MgSO_4$, filtered and concentrated under *vacuo*. The crude residue was purified via silica gel flash column chromatography. Elution with 20–50% EtOAc/hexanes afforded compound **4a** as a white solid (40.8 mg) in 55% yield. $^1$H NMR (500 MHz, $CDCl_3$) $\delta$ 1.05(*s*,3H), 1.21 (*s*, 3H), 1.50 (*s*, 3H), 1.65 (*s*, 3H), 1.77 (*s*, 3H), 1.83–1.96 (*m*, 1H), 2.25 (*s*, 3H), 2.39 (*s*, 3H), 2.44–2.50 (*m*, 1H), 2.50–2.66 (*m*, 1H), 3.48 (*d*, $J$=4.8 Hz, 1H), 3.79 (*d*, $J$=6.8 Hz, 1H), 4.19 (*d* of AB *q*, $J$=8.5 Hz, 1H), 4.30 (*d* of AB *q*, $J$=8.5 Hz, 1H), 4.38–4.43 (*m*, 1H), 4.78–4.80 (*m*, 1H), 4.94 (*d*, $J$=8.8 Hz, 1H), 5.67 (*d*, $J$=7.6 Hz, 1H), 5.76–5.78 (*m*, 1H), 6.22–6.27 (*m*, 1H), 6.92 (*d*, $J$=8.8 Hz, 1H), 7.12–7.16 (*m*, 1H), 7.35–7.69 (*m*, 10H), 7.81 (*d*, $J$=7.6 Hz, 1H), 8.06 (*s*, 1H), 8.13 (*d*, $J$=7.6 Hz, 2H); HRMS *m*/*z* calculated for $C_{47}H_{50}O_{14}NINa$: 1002.2168. Found: 1002.2119.

### 5.7. 3′-Debenzoyl-3′-(2-iodobenzoyl)paclitaxel (4c)

To a stirred solution of **3c** (80.4 mg, 0.078 mmol) in tetrahydrofuran (13 mL) and MeOH (13 mL) was added $NH_4OAc$ (60.0 mg, 0.780 mmol). After stirring at room temperature for 5 h, the reaction mixture was diluted with EtOAc, washed with brine, dried over $MgSO_4$, filtered and concentrated under reduced pressure. The crude residue was purified via silica gel flash column chromatography. Elution with 20–50% EtOAc/hexanes afforded compound **4c** as a white solid (37.1 mg) in 53% yield. $^1$H NMR (500 MHz, $CDCl_3$) $\delta$ 1.15 (*s*,3H), 1.25 (*s*, 3H), 1.65 (*s*, 3H), 1.68 (*s*, 3H), 1.84 (*s*, 3H), 1.87–1.89 (*m*, 1H), 2.24 (*s*, 3H), 2.36 (*s*, 3H), 2.38–2.56 (*m*, 2H), 3.50 (*d*, $J$=5.5 Hz, 1H), 3.79 (*d*, $J$=7 Hz, 1H), 4.20 (*d* of AB *q*, $J$=8.5 Hz, 1H), 4.30 (*d* of AB *q*, $J$=8.5 Hz, 1H), 4.37–4.42 (*m*, 1H), 4.78 (*dd*, $J$=5.5, 2 Hz, 1H), 4.92 (*d*, $J$=9 Hz, 1H), 5.67 (*d*, $J$=7 Hz, 1H), 5.75 (*m*, 1H), 6.27 (*t*, $J$=9 Hz, 1H), 6.61 (*d*, $J$=9.5 Hz, 1H), 7.07–7.10 (*m*, 1 H), 7.34–7.60 (*m*, 10 H), 7.83 (*d*, $J$=8 Hz, 1 H), 8.09 (*s*, 1 H), 8.15 (*d*, $J$=8 Hz, 2 H); HRMS *m*/*z* calculated for $C_{47}H_{50}O_{14}N1Na$: 1002.2168. Found: 1002.2188.

### 5.8. 3-(Trimethylstannyl)benzoic acid (6)

To a Schlenk flask was added 3-iodobenzoic acid (248.0 mg, 1 mmol), dioxane (2.4 mL), hexamethylditin (786 mg, 2.4 mmol), and $PdCl_2(Ph_3P)_2$ (2 mol%). The reaction mixture was degassed for 5–6 min and then heated at 70 °C for 22 h. The reaction mixture was filtered and the solvent was concentrated under reduced pressure. The crude residue was purified via silica gel flash column chromatography. Elution with 3–10% EtOAc/hexanes afforded compound **6** as a white solid (141 mg) in 50% yield. $^1$H NMR (400 MHz, $CDCl_3$) $\delta$ 0.27(*s*,9H), 7.42–7.46 (*m*, 1H), 7.72–7.74 (*m*, 1H), 8.03–8.04 (*m*, 1H), 8.22 (*s*, 1H), 8.44 (*s*, 1H).

### 5.9. 3-(Trimethylstannyl)benzoic pivalic anhydride (7)

To a stirred solution of **6** (107 mg, 0.374 mmol) in $CH_2Cl_2$ (10.6 mL) and $Et_3N$ (78.3 μL, 0.56 mmol) was added dropwise at 0 °C pivaloyl chloride (50 μL, 0.404 mmol). The reaction mixture was allowed to stir at room temperature and the reaction progress was monitored by TLC. The reaction was completed after 3 h. The solvent was removed under reduced pressure and the residue was used for the next step without further purification.

### 5.10. 3′-Debenzoyl-7-(trichloroethoxycarbonyl)-3′-(3-trimethylstannylbenzoyl)paclitaxel (8)

To a stirred solution of 3′-debenzoyl-7-(trichloroethoxycarbonyl)-paclitaxel (**2**) (88.1 mg, 0.098 mmol) in dry pyridine (9.5 mL) was added dropwise at 0 °C 3-trimethylstannylbenzoic pivalic anhydride (**7**). The reaction mixture was allowed to stir at this temperature for 3 h. The solvent was evaporated under reduced pressure and the crude residue was used for the next step without further purification.

### 5.11. 3′-Debenzoyl-3′-(3-trimethylstannylbenzoyl)paclitaxel (9)

To a stirred solution of **8** (112.4 mg, 0.096 mmol) in tetrahydrofuran (16 mL) and MeOH (16 mL) was added $NH_4OAc$ (60.0 mg, 0.77 mmol). The reaction mixture was allowed to stir at room temperature for 22 h and then the reaction mixture was diluted with EtOAc, washed with brine, dried over $MgSO_4$, filtered and concentrated under reduced pressure. The crude residue was purified via HPLC using Phenomenex Luna 10 μ Silica Column (250 × 10 mm). EtOAc/$CH_2Cl_2$ (1:1) was used an eluent. The flow rate was 4 ml/min. Compound **9** was obtained as a white solid (29.2 mg) in 30% yield. $^1$H NMR (500 MHz, $CDCl_3$) $\delta$ 0.27 (*s*,9H), 1.16 (*s*, 3H), 1.26 (*s*, 3H), 1.70 (*s*, 3H), 1.82 (*s*, 3H), 1.87 (*s*, 3H), 1.90–1.96 (*m*, 1H), 2.26 (*s*, 3H), 2.41 (*s*, 3H), 2.49–2.56 (*m*, 2H), 3.49 (*m*, 1H), 3.81 (*d*, *J*=7 Hz, 1H), 4.21 (*d* of AB *q*, *J*=8.5 Hz, 1H), 4.31 (*d* of AB *q*, *J*=8 Hz, 1H), 4.39–4.44 (*m*, 1H), 4.82 (*m*, 1H), 4.95 (*d*, *J*=8.5 Hz, 1H), 5.68 (*d*, *J*=7 Hz, 1H), 5.81–5.83 (*m*, 1H), 6.26–6.29 (*m*, 2H), 6.99 (*d*, *J*=9 Hz, 1H), 7.37–7.64 (*m*, 11 H), 7.89 (*s*, 1H), 8.14 (*d*, *J*=7.5 Hz, 2H); $^{13}$C NMR (125 MHz, $CDCl_3$) $\delta$ – 9.54, 9.56, 14.81, 20.80, 21.82, 22.62, 26.85, 35.64, 35.74, 43.67, 55.06, 58.65, 72.17, 72.34, 75.01, 75.58, 79.08, 81.18, 84.41, 126.42, 127.24, 128.72, 128.99, 129.23, 130.22, 133.12, 133.25, 133.70, 134.46, 138.06, 139.37, 141.98, 143.58, 167.01, 167.64, 170.36, 171.17, 172.72, 203.61; HRMS *m*/*z* calculated for $C_{50}H_{59}O_{14}NNaSn$: 1040.2850. Found: 1040.2860.

## 6. Radiolabeling

### 6.1. 3′-Debenzoyl-3′-(3-[$^{124}$I]iodobenzoyl)paclitaxel (10)

$Na^{124}I$ in 0.1 M NaOH (10–30 μL) was added to acetic acid (100 μL of 5%) in acetonitrile, mixed and transferred to an IODO-GEN coated tube. The stannylated precursor **9** (40 μg) was dissolved in an acetic acid/ acetonitrile (50 μL of 10%) solution and transferred to the IODO-GEN coated tube. The solution was mixed and left at room temperature for 15 min. The reaction mixture was purified on an HPLC using a Phenomenex Luna C18(2) column (4.6 × 250 mm). The eluent was 60% acetonitrile, 40% water and the flow rate was 1 mL/min. The product was collected, diluted with water and loaded onto a C18 Sep–Pak (Waters, Milford, MA). The product was eluted with ethanol. The radiochemical yield of the product was 39.9% ± 7.7%. The specific activity was found to be > 1 Ci/μmol for the labeled product. The product was assayed for radiochemical purity using Maxsil C18 analytical column (5 μ, 4.5 × 250 mm) eluted with a 70:30 mixture of methanol/$NH_4HCO_3$ at a flow rate of 1 mL/min (Fig. 2). The radiochemical purity was also analyzed using Radio-TLC developed in a 2:1 mixture of ethyl acetate and *n*-hexanes. The final product was formulated in saline: Cremophor: ethanol (5:0.5:0.5) mixture for animal studies. Cremophore/ethanol is the formulation used for paclitaxel in clinics due its insolubilty in water and saline and therefore this folmulation was used.

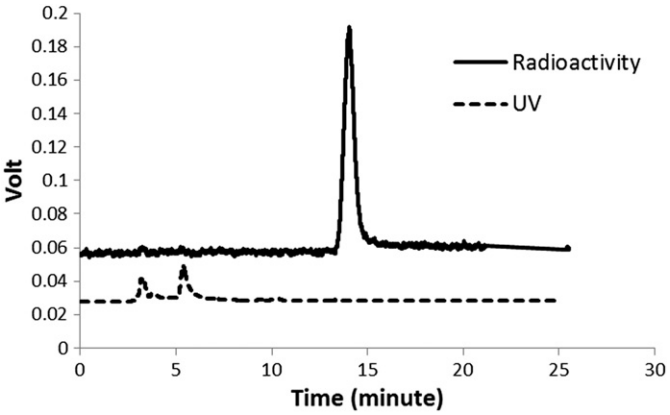


**Fig. 2.** HPLC analysis of purified 3′-debenzoyl-3′-(3-[$^{124}$I]iodobenzoyl)paclitaxel on a C18 column.

## 7. Results and discussion

### 7.1. Chemistry

The synthesis of the iodobenzoylpaclitaxel analogs **4a**–**4c** is outlined in Scheme 1. The iodinated analogs **4** were prepared from paclitaxel precursor **1,** which was synthesized, using the method of Reddy et al. (2001). The *N*,*O*-acetonide and the Boc-protecting group in precursor **1** were removed using formic acid to furnish 3′-aminopaclitaxel intermediate **2**. Reaction of the free amino group in **2** with 2-, 3-, and 4-iodobenzoyl chloride provided the three regioisomeric iodo analogs **3**. Deprotection of the Troc (trichloroethoxycarbonyl) protecting group in **3** using excess ammonium acetate at room temperature afforded the iodinated paclitaxel analogs **4**.

The trimethylstannylated paclitaxel derivative **9** (Scheme 2) was prepared following the method by Roh et al. (2000). 3-Trimethylstannylbenzoic acid was prepared by treating 3-iodobenzoic acid with hexamethylditin in the presence of a catalytic amount of the dichlorobis(triphenyl phosphine) palladium (II) complex in dioxane (Koziorowski et al., 1998). Reaction between pivaloyl chloride and 3-trimethylstannylbenzoic acid (**6**) in the presence of triethylamine provided the mixed anhydride **7**. The coupled product **8** was obtained by treating the mixed anhydride **7** with intermediate **2** in the presence of pyridine. The trimethylstannyl precursor **9** was obtained by deprotection of the Troc

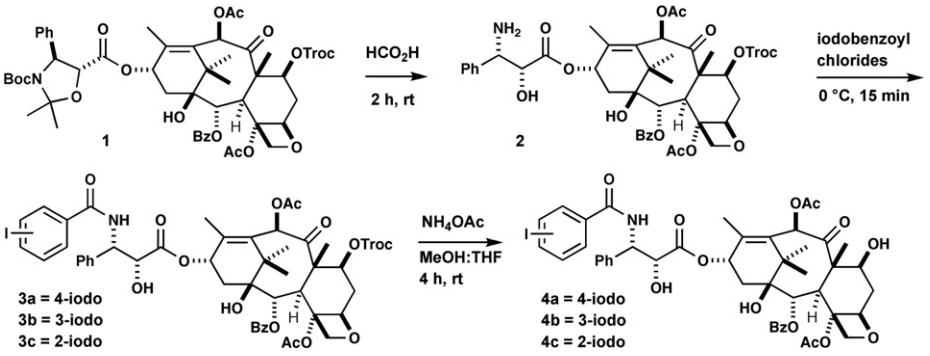


**Scheme 1.** Preparation of iodobenzoylpaclitaxel analogs **4a**–**4c**.

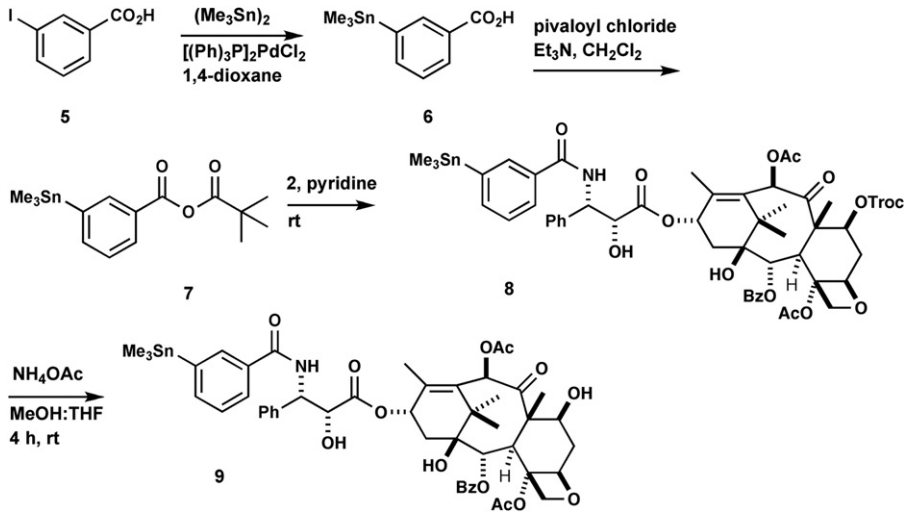


**Scheme 2.** Preparation of 3′-debenzoyl-3′-(3-trimethylstannyl)benzoylpaclitaxel (**9**).

**Table 1**
$IC_{50}$ (nM) of paclitaxel and various iodo analogs against sensitive and drug-resistant human cancer cell lines.

| Compound | MCF7(S) ($Pgp^-$) | NCI/ADR-RES ($Pgp^+$) | MDA-435/LCC6(WT) ($Pgp^-$) | MDA-435/LCC6(MDR) ($Pgp^+$) |
|---|---|---|---|---|
| Paclitaxel | $0.85 \pm 0.06$ | $204.29 \pm 26.15$ | $3.59 \pm 0.90$ | $351.36 \pm 7.96$ |
| 2-Iodopaclitaxel | $97.28 \pm 4.00$ | $3239.54 \pm 317.76$ | $118.32 \pm 3.66$ | $2195.73 \pm 252.52$ |
| 3-Iodopaclitaxel | $1.94 \pm 0.16$ | $374.64 \pm 26.28$ | $6.19 \pm 1.24$ | $536.51 \pm 14.69$ |
| 4-Iodopaclitaxel | $8.98 \pm 0.54$ | $1057 \pm 68.53$ | $10.30 \pm 0.29$ | $294\ 23 \pm 6.42$ |

*S* and *WT* indicate sensitivity to paclitaxel. ADR-RES and MDR indicate resistance to paclitaxel.

protecting group using ammonium acetate in MeOH and THF at room temperature. The $^1$H NMR and HRMS data of **9** were consistent with the literature data (Roh et al., 2000).

The effect of paclitaxel and the three iodinated paclitaxel analogs on sensitive and drug-resistant human cancer cell lines cell growth was studied. The concentration (nM) of each paclitaxel analog required to inhibit tumor cell growth by 50% ($IC_{50}$) is shown in Table 1. The tumor cell growth inhibitory activity of the 3-iodo isomer **4b** was found to most closely match the values for paclitaxel. Therefore 3′-debenzoyl-3′-(3-iodobenzoyl)paclitaxel **4b** was selected for labeling as 3′-debenzoyl-3′-(3-[$^{124}$I]iodobenzoyl)paclitaxel (**10**) (Scheme 3).

### 7.2. Radiochemistry

3′-Debenzoyl-3′-(3-[$^{124}$I]iodobenzoyl)paclitaxel (**10**) was prepared by electrophilic aromatic radioiodination of stannylated paclitaxel analog **9** with iodine-124 in the presence of Iodogen. The reaction was completed after 15 min at room temperature. The crude product was purified by high performance liquid chromatography and radioactive product **10** was obtained in 40% radiochemical yield and its specific activity was found to be $>1$ Ci/μmoL.

Biodistribution studies were performed in nude athymic mice as described in the experimental section. The data is shown in Table 2. The initial uptake of tracer was high in spleen, kidney, lungs, heart, liver and gut but is cleared significantly after 6 h from these tissues.

Fig. 3 shows the uptake of the labeled drug **10** by MDA-435/LCC6(WT) and MDA-435/LCC6(MDR) tumors implanted sc in nude mice. No significant difference is observed in uptake between resistant and sensitive tumors for the first 6 h but at 24 h post-injection the uptake and/or retention of WT cell was significantly (2.4-fold) higher than the RES line ($p < 0.0135$). Fig. 4 details the uptake in MCF7 paclitaxel-sensitive and NCI/ADR-RES resistant tumors. In this case, the same trend was observed with a higher uptake and/or retention of WT cells as compared to RES cells, observed after 6 h ($p < 0.041$) and 24 h ($p < 0.0012$)

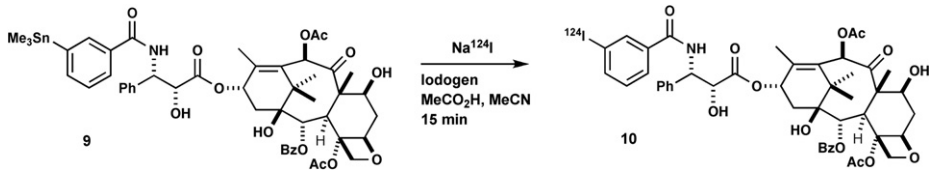


**Scheme 3.** Preparation of 3′-debenzoyl-3′-(3-[$^{124}$I]iodobenzoyl)paclitaxel (**10**).

**Table 2**
Biodistribution of $^{124}$I-paclitaxel derivative **10** in nude mice. (Average of five mice).

| Parts/ Time (h) | 0.5 | 2.0 | 6.0 | 24.0 |
|---|---|---|---|---|
| Blood | 0.83 ± 0.18 | 0.38 ± 0.21 | 0.06 ± 0.02 | 0.011 ± 0.003 |
| Muscle | 1.1 ± 0.48 | 0.9 ± 0.47 | 0.08 ± 0.02 | 0.01 ± 0.004 |
| Spleen | 2.05 ± 0.69 | 0.75 ± 0.21 | 0.12 ± 0.02 | 0.05 ± 0.012 |
| Kidney | 4.73 ± 1.29 | 1.41 ± 0.35 | 0.16 ± 0.07 | 0.042 ± 0.05 |
| Lungs | 7.5 ± 0.3.46 | 2.4 ± 0.0.87 | 0.41 ± 0.36 | 0.082 ± 0.031 |
| Heart | 1.36 ± 0.41 | 0.31 ± .09 | 0.045 ± 0.01 | 0.01 ± 0.003 |
| Liver | 20.44 ± 3.38 | 6.76 ± 1.04 | 0.79 ± 0.11 | 0.16 ± 0.03 |
| Gut | 10.12 ± 6.65 | 22.27 ± 14.39 | 1.34 ± 0.34 | 0.13 ± 0.06 |
| Stomach | 1.72 ± 0.7 | 3.2 ± 1.9 | 0.22 ± 0.21 | 0.05 ± 0.02 |

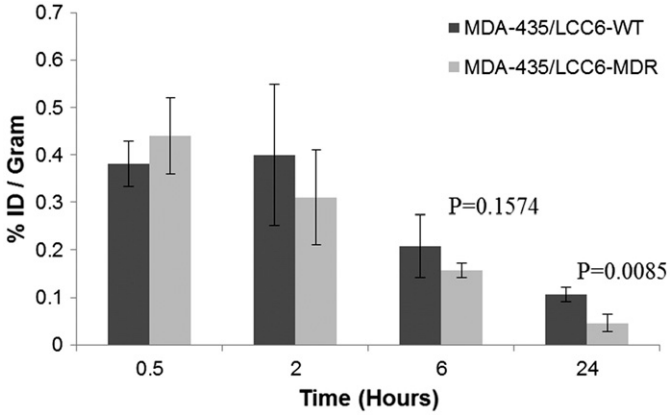


**Fig. 3.** Uptake of the labeled paclitaxel derivative **10** in nude mice with MDA-435/LCC6-WT and MDA-435/LCC6-MDR tumors.

post-injection. This differential uptake and/or retention of drug found between the 'drug sensitive' and 'drug resistant' tumors most probably is related to the differential expression of multi-drug transporters (i.e., Pgp) expressed within these pairs of tumor cell lines. The cellular degree of drug sensitivity and/or resistance to paclitaxel and its analogs were examined previously for each tumor cell lines and expressed as IC50s (the concentration of agent needed to inhibit tumor cell growth by 50%) (Table 1). The higher the $IC_{50}$ for a particular agent in a tumor cell line implies a certain degree of drug resistance to that agent. To compare the degree of drug resistance within each pair of tumor cell lines, an *R*/*S* ratio can be calculated using the $IC_{50}$ for the resistant cell line (e.g. NCI/ADR-RES) divided by that of the sensitive cell line (e.g., MCF7(S). Table 3 lists the *R*/*S* ratio of paclitaxel and the 3-iodo derivative of paclitaxel for the two pairs of tumor cell lines. Using these criteria, the NCI/ADR-RES tumor appears to be 240 fold more resistant to paclitaxel as compared with the drug sensitive MCF7(S) tumor (Table 3).

The higher the *R*/*S* value, the greater differential in Pgp expression and the faster the clearance of drug from the resistant tumor. We believe that this could explain the reason that differential drug uptake/retention was noted earlier (within 6 h) for the NCI/ADR-RES/MCF7 tumor pair than for the MDA-435/LCC6 tumor pair.

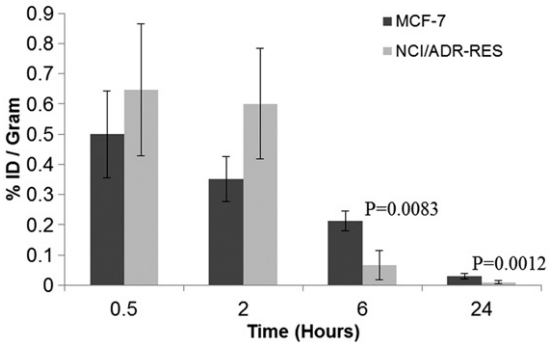


**Fig. 4.** Uptake of the labeled paclitaxel derivative **10** in nude mice with MCF-7 and NCI/ADR-RES tumors.

**Table 3**
$IC_{50}$ ratio's (resistant/sensitive) for various compounds against tumor cell lines.

| Compound | NCI/ADR-RES and MCF7 | MDA-435/LCC6(MDR) and MDA-435/LCC6(WT) |
|---|---|---|
| Paclitaxel | 240 | 98 |
| 3-Iodopaclitaxel **4b** | 193 | 87 |

In addition, the initial measurements of drug levels in the tumors may be the result of significant amounts of labeled drug in the blood and other extracellular compartments of the tumors. With time, this loading dose diminishes and later time points may reflect more accurately the amount of drug uptake and retention by tumor cells. Therefore the 24 h time points probably better reflect the action of the Pgp efflux pump, accounting for the significant lowering of drugs levels in the highly resistant, highly Pgp expressing tumor cell lines (NCI/ADR-RES and MDA-435/LCC6(MDR)).

### 7.3. Imaging

Nude mice with MDA-435/LCC6(WT) (on the left shoulder) and resistant tumors (on the right shoulder) were injected intravenously with 7.4 MBq of the $^{124}$I-labeled drug. Animals were imaged sequentially using a microPET focus 120 camera. Isoflurane was used as anesthetic agent during the imaging session. Animals were imaged after 5 min, 8 h and 24 h post-injection. Images obtained after 5 min post radioactivity injections did not show the tumors as the background activity in liver and gut was still too high. All 8 h post-injection images were also negative with an exception of one mouse where the tumor was barely visible. At 24 h post-injection the sensitive tumor was visible in four out of eight mice. Fig. 5 shows the whole-body microPET image with the sensitive tumor clearly visible on the left shoulder. The thyroid is also visible in 24 h image, which shows some dehalogenation of the compound. Fig. 5 shows that the thyroid uptake is lower than the tumor. As tumor uptake is low and the thyroid is barely visible in the 8 h post injection image, therefore it can be concluded that the dehalogenation is not very significant. In previously reported studies, Dupertuis et al. (2001) have added 0.2 g/liter of potassium iodide in the drinking water of the animals. These animals were

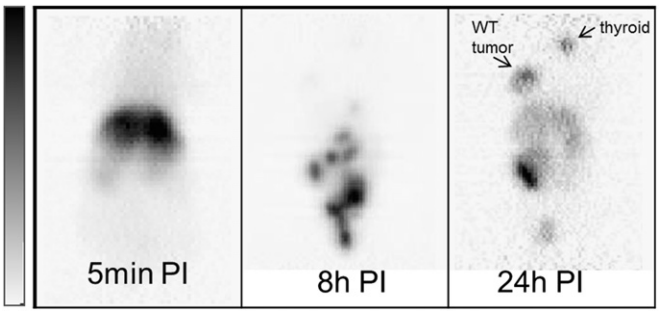


**Fig. 5.** The coronal view of images obtained with no modulator drug applied on the Focus 120 microPET (Concorde Systems Inc., Knoxville, TN). A total of 20 planes (~0.8 mm/plane) encompassing the tumor and thyroid were selected in the coronal orientation and summed. The sensitive tumor MDA-435/LCC6(WT) was on the left shoulder and the resistant tumor MDA-435/LCC6(MDR) on the right shoulder. From left to right, the three images were imaged at 5 min, 8 h and 24 h post-injection, respectively. Tracer uptake is vaguely seen in the image of 8 h post-injection in the sensitive tumor. The visibility was greatly enhanced in the 24 h post-injection image. Each image was scaled to its maximum for display.

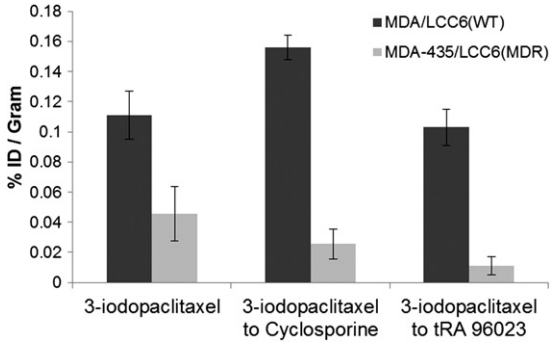


**Fig. 6.** The effect of Cyclosporine and tRA 96023 on 3′-debenzoyl-3′-(3-[$^{124}$I]iodobenzoyl)paclitaxel uptake at 24 h post-injection.

given this water 24 h prior to the administration of the drug to block thyroid uptake of the radioactive iodide present due to dehalogenation of the tracer.

The effect of Pgp-modulators Cyclosporine and tRA 96023 on tumor uptake was also studied. Cyclosporine (2 mg/kg) and tRA 96023 (4 mg/kg) were injected 1 h before the radioactive injection. Fig. 6 shows the effect of the modulators on tumor uptake.

The uptake and or retention of labeled drug increased in the drug sensitive MDA-435/LCC6(WT) tumor apparently due to the effect of Cyclosporine by 1.4 times compared to the normal uptake. There was no statistically significant effect of tRA 96023 on tumor drug uptake/retention in this tumor pair. It was noted that resistant tumor uptake/retention was decreased by 1.4 and 4.5 times compared with sensitive tumor uptake. The sensitive to resistant tumor uptake/retention ratios (*R*/*S*) for non-treated and cyclosporine and tRA 96023 pretreated mice were 2.4, 6.1 and 9.4 respectively. The Pgp modulators had a positive effect on the sensitive tumor uptake whereas they had a negative effect on the resistant tumor uptake. The modulator treated mice were imaged 24 h post-injection. The sensitive tumors of the three out of four Cyclosporine treated mice were visible whereas in the tRA 96023 treated mice the tumor was visible only in one out of three mice studied. Fig. 7 shows images of the mice treated with Cyclosporine and tRA 96023. In the Cyclosporine treated mouse, the sensitive tumor is clear compared to the tRA96023 treated mouse, which is related to its higher activity in the tumor. Low tumor uptake/retention of the drug is the reason for 50% visibility of the sensitive tumor.

We have used 3′-debenzoyl-3′-(3-[$^{124}$I]iodobenzoyl)paclitaxel to investigate the effect of low molecular weight heparins

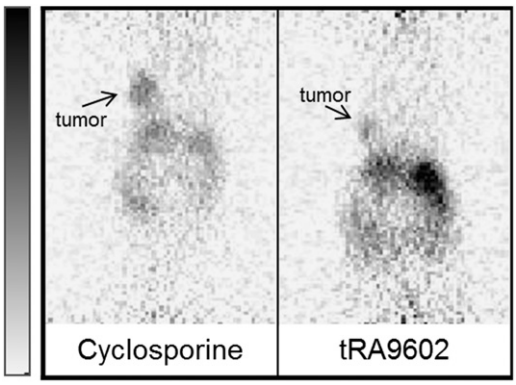


**Fig. 7.** The coronal view of images obtained with modulator drugs Cyclosporine (A) and tRA 9602 (B) applied. A total of 8 planes (~0.8 mm/plane) encompassing the tumor were selected in the coronal orientation and summed. Both images were obtained at 24 h post-injection. The sensitive tumors MDA-435/LCC6(WT) in both mice are visible in the images.

(LMWHs) tinzaparin and a sulfated non-anticoagulant LMWH (S-NACH) on tumor chemotherapeutic uptake and chemoresponse. LMHW increased 3′-debenzoyl-3′-(3-[$^{124}$I]iodobenzoyl)-paclitaxel uptake into MDA453/LCC6 tumors, with tumor to muscle ratios several fold greater than that of 3′-debenzoyl-3′-(3-[$^{124}$I]iodobenzoyl)paclitaxel alone at 24 h post–injection (Phillips et al. (2011). Similarly, LMWH and S-NACH significantly increased the uptake of doxorubicin (Dox) by 1.5-2 fold in NCI/ADR-RES Dox resistant tumor xenografts. The above study shows that 3′-debenzoyl-3′-(3-[$^{124}$I]iodobenzoyl)paclitaxel is a useful tracer for studying the effect of other agents on potentially overcoming paclitaxel tumor chemoresistance. The next experiment under planning is to study the uptake of this tracer in SCID mice implanted with human breast or lung tumor.

## 8. Summary

3′-Debenzoyl-3′-(3-iodobenzoyl)paclitaxel was found to match most closely paclitaxel when compared to the other isomers in antiproliferative assays. The 3′-debenzoyl-3′-(3-[$^{124}$I]iodobenzoyl)paclitaxel analogs were prepared by aromatic iodination of 3-debenzoyl-3′-(3-trimethylstannylbenzoyl)paclitaxel. The uptake of the labeled drug was higher in sensitive tumors compared to the resistant tumors. Application of Pgp-modulators Cyclosporine increased drug accumulation in drug-sensitive tumors where as tRA 96203 effects were not very significant. Both modulators had a negative effect on Pgp-expressing tumors. The analog 3′-debenzoyl-3′-(3-iodobenzoyl)-paclitaxel seems to accurately predict the activity of Pgp in tumor cells, therefore it may have the potential of determining if a particular tumor type may be responsive or resistant to treatment with paclitaxel, helping oncologists to determine the most appropriate therapy for that patient, adhering to the concept of personalized medicine.

## Acknowledgment

This work was supported by an award from the Roswell Park Alliance Foundation.

## References

Brooks, T., Minderman, H., O'Louglin, K., Pera, P., Ojima, I., Baer, M., Bernacki, R.J., 2003. Taxane-based reversal agents modulate drug resistance mediated be P-glycoprotein, multidrug resistance protein and breast cancer resistance protein. Mol. Cancer Ther. 2, 1195–1205.

Dupertuis, Y.M., Vazquez, M., Mach, J.P., Tribolet, N.D., Pichard, C., Slosman, D.O., Buchogger, F., 2001. Fluorodeoxyuridine Improves Imaging of Human Glioblastoma Xenografts with radiolabeled Iododeoxy Uridine. Cancer Res. 61. 7971-7077.

Gottesman, M.M., Fojo, T., Bates, S.E., 2002. Multidrug resistance in cancer: Role of ATP-dependent transporter. Nature Rev. Cancer 2, 48–58.

Hendrikse, N.H., Vaalburg, W., 2002. Dynamics of multidrug resistance: P-glycoprotein analysis with positron emission tomography. Methods 27, 228–233.

Holford, N.H.G., Scheiner, L.B., 1981. Understanding the dose-effect relationship: Clinical applications of pharmacokinetic-pharmacodynamic models. Clin. Pharmocokinet 6, 429–453.

Kiesewetter, D.O., Jagoda, E.M., Kao, C.K., Ma, Y., Ravasi, L., Shimoji, K., Szajek, P., Eckelman, C., 2003. Flouro-, bromo, and iodopaclitaxel derivatives: synthesis and biological evaluation. Nucl. Med. Biol. 30, 11–24.

Koziorowski, J., Henssen, C., Weinreich, R., 1998. A new convenient route to radioiodinated N-succinimidiyl 3- and 4-iodobenzoate, two reagents for radioiodination of proteins. Appl. Radiat. Isot 49, 955–959.

Li, C., Yu, D.F., Inoue, T., Yang, D.J., Tansey, W., Lui, C.W., Milas, L., Hunter, N.R., Kim, E.E., Wallace, S., 1997. Synthesis, biodistribution and imaging properties of indium-111-DTPA-paclitaxel in mice bearing mammary tumors. J. Nucl. Med. 38, 1042–1047.

Marquardt, D.W., 1963. An algorithm for least squares estimation of nonlinear parameters. J. Soc. Indust. Appl. Math 11, 431–441.

Nash, J.C., 1979. Compact Numerical Method for Computers: Linear Algebra and Function Minimization. John Wiley & Sons, New York.

Phelps, M.E., 2000. Positron emission tomography provides molecular imaging of biological processes. Proc. Nat. Acad. Sci. U.S.A. 97, 9226–9233.

Phillips, P.G., Yalcin, M., Cui, H., Abdel-Nabi, H., Sajjad, M., Bernacki, R., Veith, J., Mousa, S.S., 2011. Increased Tumor Uptake of Chemotherapeutics and Improved Chemoresponse by Novel Non-anticougulant Low Molecular weight Heparin. Anticancer Res. 31, 411.

Reddy, S.H.K., Lee, S., Datta, A., George, G.I., 2001. Efficient synthesis of the 3′-phenolic metabolite of paclitaxel. J. Org. Chem. 66, 8211–8214.

Roh, E.J., Park, Y.H., Song, C.E., Oh, S.J., Choe, Y.S., Kim, B.T., Chi, D.Y., Kim, D., 2000. Radiolabeling of paclitaxel with electrophilic $^{123}$I. Bioorg. Med. Chem. 8, 65–68.

Sajjad, M., Bars, E., Nabi, H.A.J., 2006. Optimization of $^{124}$I production via $^{124}$Te(p,n)$^{124}$I reaction. Appl. Radiat. Isot 64, 965–970.

Skehan, P., Storeng, R., Scudiero, D., Monks, A., McMohan, J., Vistica, D., et al., 1990. New Colorimetric Cytotoxicity Assay for Anticancer-Drug Screening. J. Natl. Cancer Inst. 82, 1107–1112.

Vredenburg, M.R., Ojima, I., Veith, J., Pera, P., Kee, K., Cabral, F., Sharma, A., Kanter, P., Bernacki, R.J., 2001. Orally-active taxanes which modulate P-glycoprotein, overcoming resistance in colon and breast carcinomas. J. Natl. Cancer Inst. 93, 1234–1245.